Available online at www.sciencedirect.com
SCIENCE DIRECT®
Journal of Nuclear Materials 340 (2005) 113–118
journal of nuclear materials
www.elsevier.com/locate/jnucmat

Letter to the Editors

Densification behaviour and sintering kinetics of $(U_{0.45}Pu_{0.55})C$ pellets

T.R.G. Kutty [a,*], K.B. Khan [a], P.S. Kutty [a], C.B. Basak [a], A.K. Sengupta [a], R.S. Mehrotra [a], S. Majumdar [a], H.S. Kamath [a,b]

[a] *Radiometallurgy Division, Bhabha Atomic Research Centre, Trombay, Mumbai 400 085, India*
[b] *Nuclear Fuels Group, Bhabha Atomic Research Centre, Trombay, Mumbai 400 085, India*

Received 16 September 2004; accepted 1 November 2004

Abstract

The sintering behaviour of $(U_{0.45}Pu_{0.55})C$ pellets has been studied up to 1700 °C using a dilatometer in Ar–8%H_2 atmosphere. The mechanism for the initial stage of sintering was determined using rate controlled sintering technique and was found to be volume diffusion. The activation energy for the initial stages of sintering was found to be 360 kJ/mol for Ar–8%H_2 atmosphere.

PACS: 81.20.Ev; 82.20.Pm; 61.72.−y; 66.30.Fq

1. Introduction

The Fast Breeder Test Reactor (FBTR) at the Indira Gandhi Centre for Atomic Research, Kalpakkam is the first of its kind in the world that uses uranium–plutonium mixed carbide as driver fuel. FBTR was made critical with a small compact core consisting of Pu-rich hyperstoichiometric $(U_{0.3}Pu_{0.7})C$ fuel (Mark-I) which has already reached a burn-up of 100 000 MW days per ton without any pin failure [1–3]. The core is now being expanded with hyperstoichiometric $(U_{0.45}Pu_{0.55})C$ fuel (Mark-II) for the operation at full power. The FBTR has provided valuable experience with Liquid Metal Fast Breeder Reactor (LMFBR) technology and given confidence to set up a 500 MWe Prototype Fast Breeder Reactor (PFBR).

The fuel for the above reactor is in the form of pellets and is fabricated by powder metallurgy technique. The fabrication steps include carbothermic reduction of a homogeneous blend of UO_2, PuO_2 and graphite powders in vacuum at about 1475 °C [1–4]. The carbide clinker thus obtained is then milled, precompacted, granulated and finally compacted at 400 MPa. The sintering of the green pellets is carried out in Ar–8%H_2 at 1650 °C for 4 h [1]. The final product always contained residual oxygen as impurity in varying amounts depending up on the fabrication condition [2,3]. As the overall carbon-to-metal ratio of the fuel matrix decreases with increasing burn-up of the fuel on account of the fact that the fission products tie up with more carbon than the actinide atoms, there is a possibility of the metal phase formation in the fuel with increased burn-up. Hence,

* Corresponding author. Tel.: +91 22 2550 5151; fax: +91 22 2559 5361.
E-mail address: tkutty@magnum.barc.ernet.in (T.R.G. Kutty).

0022-3115/$ - see front matter © 2004 Elsevier B.V. All rights reserved.
doi:10.1016/j.jnucmat.2004.11.007

to avoid the formation of metallic phase which has a low melting point, the mixed carbide fuels are designed to be slightly hyperstoichiometric and fabricated to exist in the phase field of MC + M_2C_3 (M = U + Pu). Since the commercial carbide fuel usually contains more than 2500 ppm of oxygen, a detailed investigation of U–Pu–C–O system is an essential prerequisite for optimizing the parameters of fuel pellets production. In the M–C–O system, the M(C, O) + M_2C_3 phase field is the most important. Oxygen dissolved in the monocarbide phase forms $M(C_{1-x}, O_x)$, which is nothing but a solid solution of (MO) in MC [5]. The lattice parameter of M(C, O) decreases with increase in oxygen content. It has been observed that M_2C_3 phase, in carbon rich M(C, O), becomes enriched in Pu [2,5,6].

The purpose of this study is to evaluate the densification behaviour of $(U_{0.45}Pu_{0.55})C$ pellets and determine the kinetics of sintering using rate controlled sintering technique [7,8].

2. Rate controlled sintering (RCS)

In this technique, the green compact is heated in a dilatometer at a constant heating rate until dl/dt i.e. slope of the length change versus time curve, becomes larger than a threshold value, at which point the temperature rise is stopped. The shrinkage now takes place under isothermal condition. On completion of sintering at this temperature, which is shown by the smaller dl/dt signal than a second threshold value, the temperature rise is resumed and the process is repeated. The experimental shrinkage curve obtained by dilatometry generally follows an equation of the form [9]:

$$\Delta l/l_0 = Y = [K(T)t]^n, \tag{1}$$

where l_0 is the initial length of sample at the start of sintering, $K(T)$ is Arrhenius constant, t is the time and n is a constant whose value depends on the sintering mechanism.

If only the volume diffusion from grain boundary is operative, then the shrinkage rate is given by

$$\dot{Y} = n(5.34\gamma\Omega D_v/kTa^3)^n t^{(n-1)}, \tag{2}$$

where $n = 0.49$.

Similarly for grain boundary diffusion alone

$$\dot{Y} = n(2.14\gamma\Omega b D_b/kTa^4)^n t^{(n-1)}, \tag{3}$$

where $n = 0.33$.

In Eqs. (2) and (3), γ is the surface tension, Ω is the vacancy volume, D_v and D_b are the diffusion coefficients for volume and grain boundary respectively, T is the temperature, a is the particle radius, b is the thickness of the grain boundary and k is the Boltzmann constant. The slope of the plot of $\ln \dot{Y}$ versus $\ln t$ will be $(n-1)$ from which the sintering exponent 'n' can be evaluated. From the value of intercepts, the diffusion coefficient can be evaluated.

3. Experimental

3.1. Fabrication of green pellet

The green pellets for this study were prepared by the conventional powder metallurgy technique using UO_2, PuO_2 and graphite powders as the starting materials and consisted of the following steps:

- milling of UO_2, PuO_2 and graphite powder mixture in a planetary ball mill for 12 h,
- preparation of tablets of above powder by compaction at 75 MPa,
- Carbothermic reduction of the above tablets in vacuum (1 Pa) at 1475 °C,
- crushing the clinkers and milling in a planetary ball mill using tungsten carbide balls,
- precompaction at 150 MPa,
- granulation of the precompacts,
- final cold compaction of the granulated powder at 400 MPa into green pellets.

To facilitate compaction and to impart handling strength to the green pellets, 1 wt% each of zinc behenate and naphthalene was added as lubricant/binder during the last 1 h of the mixing/milling procedure. The green pellets were about 4.6 mm in diameter and around 7 mm in length. The characteristics of the starting (U, Pu)C powders used in this study are given in Table 1.

3.2. Dilatometry

The shrinkage behaviour of the $(U_{0.45}Pu_{0.55})C$ compacts was studied in axial direction using a push rod type horizontal dilatometer. The pellet was placed in a special

Table 1
Characteristics of starting $(U_{0.45}Pu_{0.55})C$ powders

Property	Value for $(U_{0.45}Pu_{0.55})C$
O_2 (ppm)	4903
N_2 (ppm)	448
C (wt%)	5.04
M_2C_3 content (wt%)	24
Green density (% TD)	65
C/M ratio	1.14
Theoretical density, ρ (g/cm^3)	13.62
Surface energy, γ (erg/cm^2)	570
Particle radius[a], a (A)	97
Specific surface area, S (m^2/g)	0.26

[a] $a = 6/(2\cdot\rho\cdot S\cdot f)$ where f is the shape factor.

holder made up of graphite, inside a moveable furnace. To avoid any carbon pick up, zirconia supports were placed under the pellet as well as at both ends. A push-rod placed directly against the zirconia support, which was in touch with the carbide pellet, transmitted length change to a linear variable displacement transducer (LVDT) which was maintained at a constant temperature by means of water circulation from a constant temperature bath. The accuracy of the measurement of change in length was within ±0.1 μm. The temperature was measured using a calibrated thermocouple, which was placed directly above the sample. A small force of 0.2 N was applied to the sample through the push rod. The dilatometric experiments were carried out in Ar–8%H_2 atmosphere using a flow rate of 18 l/h and a heating rate of 6 °C/min. Two pellets of $(U_{0.45}Pu_{0.55})C$ were evaluated by dilatometry. One was used to measure the shrinkage from room temperature to 1700 °C and the other was used for studying the sintering kinetics using RCS. For RCS, the temperature programme was modified in such a way that the whole sintering took place between two shrinkage rates.

Table 2
Analysis result of $(U_{0.45}Pu_{0.55})C$ pellet after sintering

Elements	Amount present	Specified value
Pu (wt%)	54.740	Pu + U + Am = 95% (max)
U (wt%)	39.330	
Am (wt%)	0.050	
C (wt%)	4.680	5.03 (max)
O_2 (ppm)	4185	5000 (max)
N_2 (ppm)	603	2000 (max)
M_2C_3 content (wt%)	18.90	5–20
Total impurity (ppm)	953	3000 (max)

Table 3
Metallic impurities in sintered $(U_{0.45}Pu_{0.55})C$ pellet

Element	Impurity (ppm)
B	0.2
Ca	20
Na	10
Al	40
Mg	50
Mn	8
Si	390
Fe	36
Cd	0.2
Cr	10
Co	10
Cu	8
Ni	20
Mo	20
Pb	20
V	10
W	160
Zn	100

3.3. Characterisation

The $(U_{0.45}Pu_{0.55})C$ pellets sintered in Ar–8%H_2 atmosphere were characterised in terms of their density and phase content. Carbon, oxygen, nitrogen and impurity contents of the pellet were evaluated. The phase content was estimated by X-ray diffractometry. Table 2 gives the typical values of carbon, oxygen, nitrogen contents of a sintered pellet and its density. The X-ray diffraction patterns of the pellets were obtained by using the Cu-K_α radiation and graphite monochromator. Typical impurity contents of $(U_{0.45}Pu_{0.55})C$ sintered pellets are shown in Table 3.

4. Results

Fig. 1 shows the shrinkage behaviour of $(U_{0.45}Pu_{0.55})C$ in Ar–8%H_2 from 400 to 1700 °C. The curve is smooth up to 1200 °C showing only expansion. From 1200 °C to 1400 °C, an increase in expansion was noticed in the shrinkage curve. It can be seen from Fig. 1 that the onset of shrinkage occurs at 1450 °C. The shrinkage continues smoothly up to 1700 °C except with a slight change in the slope in the region of 1600–1650 °C. The corresponding shrinkage rates (dl/dt) of the above pellet are shown in Fig. 2. X-ray diffraction (XRD) pattern of $(U_{0.45}Pu_{0.55})C$ pellets sintered in Ar–8%H_2 showed the presence of two phases – one is isostructural with fcc MC and the other is isostructural with bcc M_2C_3 (see Fig. 3).

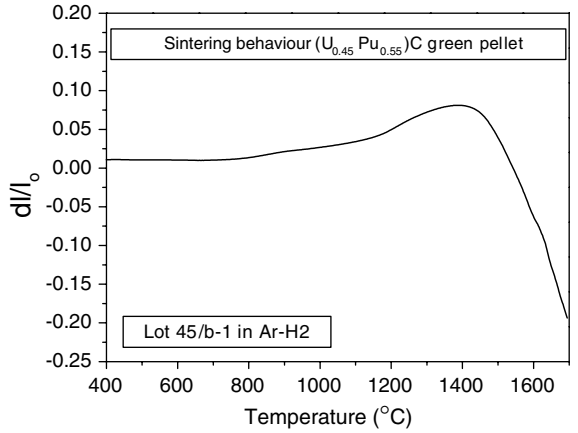

Fig. 1. Shrinkage curve for $(U_{0.45}Pu_{0.55})C$ pellet in Ar–8%H_2. The dl/l_0 values are plotted against temperature, where l_0 is the initial length.

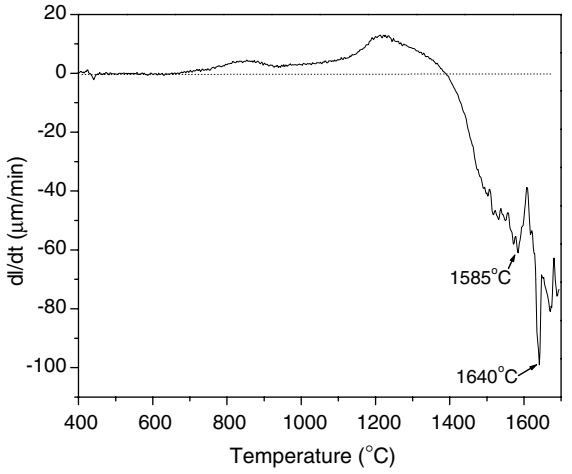

Fig. 2. Shrinkage rate (d*l*/d*t*) of $(U_{0.45}Pu_{0.55})C$ pellet plotted against temperature.

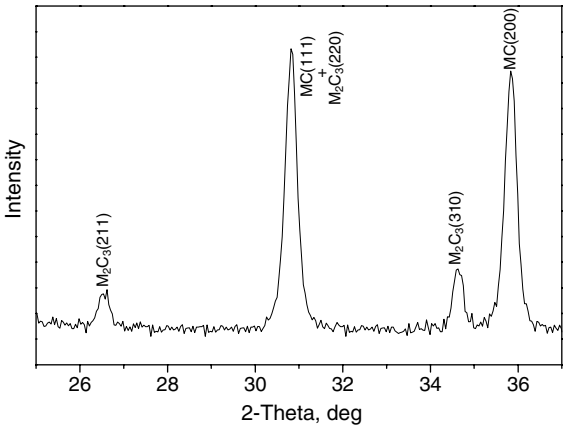

Fig. 3. XRD pattern of $(U_{0.45}Pu_{0.55})C$ pellet sintered in Ar–8%H_2.

5. Discussion

From the above result, it is evident that the onset of shrinkage in $(U_{0.45}Pu_{0.55})C$ pellets occurs at around 1450 °C. At 1700 °C, the shrinkage was about 20% (see Fig. 1). The maximum shrinkage rate of about 100 μm/min has been obtained at around 1640 °C.

Fig. 1 shows an expansion in the shrinkage curve in the temperature region of 1200–1400 °C. Let us examine the causes of the above. The following phenomena are occurring during the sintering of (U, Pu)C pellets (see Tables 1 and 2), viz.,

1. decrease in M_2C_3 content,
2. decrease in oxygen content,
3. increase in nitrogen content.

It has been noticed from Tables 1 and 2 that M_2C_3 content of the pellet has decreased from 24% before sintering to 18% after sintering. Since the sintering of the pellet has been carried out in Ar–8%H_2, M_2C_3 present in the pellet reacts with H_2 to form methane as per the following equation [10]:

$$M_2C_3 + 2H_2 \rightarrow 2MC + CH_4 \quad (4)$$

The rate of the above reaction reaches maximum at 850–900 °C. The change in the slope in the shrinkage rate curve, shown in Fig. 2, in the temperature range of 750–925 °C may be due to this reaction.

As mentioned earlier, both nitrogen and oxygen go to the lattice of carbide since they have large solubility in MC. The oxygen content of the pellet has decreased by about 800–900 ppm during the sintering. On the other hand, nitrogen content has increased by 200–300 ppm (see Tables 1 and 3). Jain and Ganguly [2] have systematically evaluated the oxygen solubility in M(C, O) phase. They have shown that M(C, O) phase in M(C, O) + M_2C_3 phase mixture is stoichiometric irrespective of oxygen content, whereas M_2C_3 phase exhibits some hypostoichiometry at low oxygen contents. The segregation of Pu occurs in M_2C_3 phase of the M(C, O) + M_2C_3 phase mixture. The extent of segregation decreases with increase of oxygen in M(C, O) phase. The following relationship has been derived between lattice parameter of M(C, O) and its (MO) content [2]:

$$\text{Lattice parameter of } M(C,O) = 0.4979 - 0.41 \times 10^{-4} \times \text{mol\% (MO)}. \quad (5)$$

Richter et al. have observed that CO evolution is maximum in the temperature range of 1000–1500 °C [11,12]. In this temperature range, we have noticed that the vacuum level of the furnace is poor indicating the release of gases. Since oxygen in the lattice of MC reacts with carbon to form CO, the net oxygen and carbon contents of the pellet decrease. Since MCO → MC reaction results in an increase in lattice parameter, the expansion observed in the shrinkage curve of $(U_{0.45}Pu_{0.55})C$ pellet is due to this reaction. To sum up, in the temperature range of 1200–1400 °C, the oxygen content of the pellet decreases and therefore the lattice expands as per Eq. (5). The expansion in the shrinkage curve (Fig. 1) is due to this phenomenon.

6. Kinetics of sintering

The sintering kinetics of $(U_{0.45}Pu_{0.55})C$ pellet has been evaluated in a reducing (Ar–8%H_2) atmosphere for the initial stages of sintering. The kinetics has been evaluated over a small temperature range of 1365–1508 °C. This temperature range was chosen from the corresponding shrinkage curve shown in Fig. 1.

The parameter 'n' of Eq. (1) is obtained from the slope of $\log \dot{Y}$ versus $\log t$ plot, shown in Fig. 4, for Ar–8%H_2 atmosphere. The value of n obtained for pellets sintered in Ar–8%H_2 is ~0.50. It was noted that the value of n was around 0.7–0.8 during the first few minutes of shrinkage. A similar phenomenon has been reported by Kutty et al. [13] for their studies on PuO_2. This may be due to the fact that the sample may not be reaching thermal equilibrium immediately after attaining the measured temperature. Hence first several points of the data were discarded and not used in this study.

The literature available on the sintering kinetics of (U, Pu)C is scanty although many reports are available on sintering kinetics of (U, Pu)O_2. Pickles et al. [14] have determined the sintering kinetics of (U, Pu)C pellets of different stoichiometries using various theoretical models available in the literature. They found that the shrinkage rates of both UC and (U, Pu)C match reasonably well with those calculated on the basis of bulk diffusion mechanism. They used a relation between shrinkage ($\Delta l/l_0$) and time t, which is given below [15]:

$$\Delta l/l_0 = [(A/T)\exp(-Q/RT)]^m t^m, \quad (6)$$

where m and A are constants for a given process in a given material. They conducted the experiments on UC, as well as on stoichiometric, hypostoichiometric and hyperstoichiometric (U, Pu)C containing 5% and 30% M_2C_3 and having a nominal composition of ($U_{0.85}Pu_{0.15}$)C [14]. The exponent, m, obtained from the slope of $\ln(\Delta l/l_0)$ versus $\ln t$ was found to vary in the range of 0.4–0.6 with a mean of 0.519, with carbide composition and sintering temperature [14]. They postulated that the sintering occurs by volume diffusion for all the carbide compositions studied. Similar studies on the shrinkage behaviour of (U, Pu)(C, N) exist in literature [16]. The value of m obtained from the shrinkage versus time plots, was found to be 0.40 suggesting the rate controlling mechanism to be volume diffusion.

The diffusion coefficients are calculated from the intercepts in Fig. 4 using Eqs. (2) and (3). The values of parameters used for this calculation are given in Table 1. The $\ln D$ versus $1/T$ plots for Ar–8%H_2 atmospheres are given in Fig. 5. The activation energy obtained for ($U_{0.45}Pu_{0.55}$)C in Ar–8%H_2 is 360 kJ/mol. There is no report available in the literature about the activation energy for ($U_{0.45}Pu_{0.55}$)C, although activation energy values are available for lower Pu compositions. The activation energy of sintering for (U, Pu)C containing <20% PuC determined from dilatometric experiments showed a marked variation from 210 to 347 kJ/mol [5].

The mechanisms of diffusion in UC and MC fuels are reported to be identical [17–19]. The predominant defects in MC fuels are metalloid C Frenkel defects. Significant amounts of vacancies are observed in UC_{1-x} and of C_2 pairs in UC_{1+x}. The thermal defect concentration is found to be less than 2% at 2125 °C. The activation energy for Pu diffusion, which depends up on C/M ratio and nitrogen content, lies in the range of 377–640 kJ/mol [20]. An Arrhenius equation for the commercial MC containing about 600 ppm of oxygen and 200 ppm of nitrogen, has been suggested which is given below [5]:

$$D = 0.013x\exp(-401\,950/RT)\ \mathrm{cm^2\ s^{-1}}. \quad (7)$$

Since the fuel covered in the present study contained much higher amount of oxygen and nitrogen, a comparison is difficult to make. However, it is noted that the value of activation energy obtained in this study (360 kJ/mol) falls very close to the reported values for the plutonium bearing mixed carbides of other compositions.

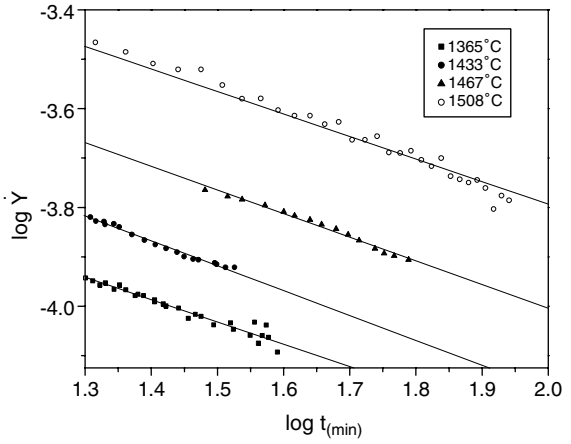

Fig. 4. A plot of $\ln \dot{Y}$ versus $\ln t$ for the pellet sintered in Ar–8%H_2. The slope of this curve will be $(n-1)$ from which the sintering exponent 'n' can be evaluated.

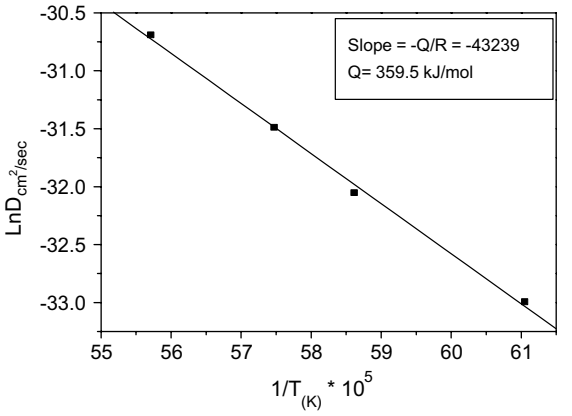

Fig. 5. The Arrhenius plot $\ln D$ versus $1/T$ for ($U_{0.45}Pu_{0.55}$)C pellet sintered in Ar–8%H_2. The slope of this curve will be Q/R from which the activation energy Q can be estimated.

7. Conclusions

The sintering behaviour of $(U_{0.45}Pu_{0.55})C$ pellet was studied with the help of a high temperature dilatometer from ambient to 1700 °C in reducing atmosphere. The following conclusions were drawn:

1. The onset of shrinkage of $(U_{0.45}Pu_{0.55})C$ pellet occurs at 1450 °C in Ar–8%H_2.
2. The expansion in the shrinkage curve in the temperature range of 1200–1400 °C may be due to the reduction in the oxygen content of the pellet during sintering.
3. The mechanism for the initial stage of sintering was considered to be volume diffusion.
4. The activation energy for sintering was found to be 360 kJ/mol for Ar–8%H_2 atmosphere.

Acknowledgments

The authors are grateful to Dr G.C. Jain and Messers U. Basak and P.V. Hegde for useful discussions and to Messers J. Banerjee, T. Jarvis, S. Mishra, S.K. Sharma and K.S. Bhatnagar for their support during the course of this work.

References

[1] C. Ganguly, P.V. Hegde, G.C. Jain, U. Basak, R.S. Mehrotra, S. Majumdar, P.R. Roy, Nucl. Tech. 72 (1986) 59.
[2] G.C. Jain, C. Ganguly, J. Nucl. Mater. 207 (1993) 169.
[3] C. Ganguly, Studies on the preparation and sintering of mixed uranium–plutonium mixed monocarbide, mononitride and monocarbonitride, PhD thesis, University of Calcutta, 1980.
[4] A.K. Sengupta, J. Banerjee, T. Jarvis, T.R.G. Kutty, K. Ravi, S. Majumdar, Nucl. Tech. 142 (2003) 260.
[5] Hj. Matzke, Science of Advanced LMFBR Fuels: A Monograph on Solid State Physics, Chemistry and Technology of Carbides, Nitrides and Carbonitrides of Uranium and Plutonium, North Holland, Amsterdam, 1986.
[6] F. Anselin, G. Dean, R. Lorenzelli, R. Pascard, in: L.E. Russell, B.T. Bradbury, J.D.L. Harrison, H.J. Hedger, P.G. Mardon (Eds.), Carbides in Nuclear Energy, Macmillan, London, 1964, p. 113.
[7] H. Palmour III, T.M. Hare, Rate-controlled Sintering Revisited, 6th Round Table Conf. on Sintering, Plenum, 1987, p. 16.
[8] H. Palmour, Sci. Sintering 7 (1989) 337.
[9] D.L. Johnson, J. Appl. Phys. 40 (1969) 192.
[10] B.R. Harder, J. Read, R.G. Sowden, J. Nucl. Mater. 17 (1965) 203.
[11] K. Ritchter, K. Kramer, J.F. Gueugnon, Trans. Am. Nucl. Soc. 31 (1979) 213.
[12] K. Ritchter, M. Coquerelle, J. Gabolde, P. Werner, Fuel and Fuel Elements for Fast Reactors, Vol. 1, IAEA, Vienna, 1974, p. 71.
[13] T.R.G. Kutty, K.B. Khan, P.V. Hegde, A.K. Sengupta, S. Majumdar, D.S.C. Purushotham, J. Nucl. Mater. 297 (2001) 120.
[14] S. Pickles, G. Yates, J.I. Bramman, M.B. Finlayson, J. Nucl. Mater. 89 (1980) 296.
[15] Hj. Matzke, J. Chem. Soc. Faraday Trans. 86 (1990) 1243.
[16] Hj. Matzke, M.H. Bradbury, Commission of the European Communities, Joint Research Centre, Karlsruhe, EUR-5906, 1978.
[17] Hj. Matzke, J.L. Routbort, H.A. Tasman, J. App. Phys. 45 (1974) 5187.
[18] J.R. Mathews, J. Nucl. Mater. 87 (1979) 356.
[19] R.J. Guenther, K.L. Petticord, in: E.C. Norman (Ed.), Proceedings of the International Conference Fast Breeder Reactor Fuel Performance, Monterey, American Nuclear Society, 1979, p. 333.
[20] Hj. Matzke, in: A.L. Laskar (Ed.), Diffusion in Materials, Kluwer Academic, Netherlands, 1990, p. 429.